PERGAMON

International Journal of Solids and Structures 40 (2003) 3089–3105

INTERNATIONAL JOURNAL OF SOLIDS and STRUCTURES

www.elsevier.com/locate/ijsolstr

Three-dimensional vibration analysis of circular and annular plates via the Chebyshev–Ritz method

D. Zhou [a,*], F.T.K. Au [b], Y.K. Cheung [b,*], S.H. Lo [b]

[a] Department of Mechanics and Engineering Science, Nanjing University of Science and Technology, Nanjing 210014, People's Republic of China

[b] Department of Civil Engineering, The University of Hong Kong, Hong Kong

Received 19 April 2002; received in revised form 9 February 2003

Abstract

A three-dimensional free vibration analysis of circular and annular plates is presented via the Chebyshev–Ritz method. The solution procedure is based on the linear, small strain, three-dimensional elasticity theory. Selecting Chebyshev polynomials which can be expressed in terms of cosine functions as the admissible functions, a convenient governing eigenvalue equation can be derived through the Ritz method. According to the geometric properties of circular and annular plates, the vibration is divided into three distinct categories: axisymmetric vibration, torsional vibration and circumferential vibration. Each vibration category can be further subdivided into the antisymmetric and symmetric ones in the thickness direction. Convergence and comparison study demonstrated the high accuracy and efficiency of the present method. The present approach shows a distinct advantage over some other Ritz solutions in that stable numerical operation can be guaranteed even when a large number of admissible functions is employed. Therefore, not only lower-order but also higher-order eigenfrequencies can be obtained by using sufficient terms of the Chebyshev polynomials. Finally, some valuable results for annular plates with one or both edges clamped are given and discussed in detail.

Keywords: Annular plates; Chebyshev–Ritz method; Circular plates; Eigenfrequency; Elasticity solution; Three-dimensional vibration

1. Introduction

As one of the most common type of structural elements, a solid or annular circular plate can find wide application in civil, mechanical, aircraft and marine engineering. Numerous investigations on the dynamic characteristics of circular plates are available in the literature. In a famous monograph, Leissa (1969) gave a systematic summary of the early investigations on free vibration of circular plates. It has been observed that the research work was mainly focused on thin plates, based on two-dimensional classical plate theory (CPT). Due to the Kirchhoff hypothesis (i.e. the hypothesis of straight normal), the CPT always

* Corresponding authors.
E-mail address: hreccyk@hkucc.hku.hk (Y.K. Cheung).

doi:10.1016/S0020-7683(03)00114-8

overestimates the eigenfrequencies and the error increases with plate thickness. Incorporating the effects of transverse shear deformation and rotary inertia, Deresiewicz and Mindlin (1955) presented the first-order shear deformable plate theory (FSDPT) which improves the accuracy of CPT solutions, especially for moderately thick plates. Moreover, some higher-order shear deformable plate theories (HSDPT) (Reddy, 1984; Hanna and Leissa, 1994) have also been developed. A review article (Liew et al., 1995) about thick plate vibration provides a comprehensive account of the relevant developments.

Two-dimensional theories reduce the dimensions of problems from three to two by introducing some assumptions in mathematical modeling. This results in relatively simple expressions and derivation of solutions. However, these simplifications inherently bring about errors and therefore theories such as CPT and FSDPT cannot avoid overlooking certain eigenfrequencies for thicker plates. As a result, three-dimensional (3D) analysis of plates has long been a goal for those who work in the field. Such an analysis not only provides realistic results but also allows further physical insights, which cannot otherwise be predicted by the two-dimensional analysis. In the recent two decades, some attempts have been made for three-dimensional vibration analysis of circular plates. Hutchinson (1979) provided a Mathieu series solution for thick, circular plates with free edges and evaluated the validity of the FSDPT (Hutchinson, 1984). Furthermore, Hutchinson and El-Azhari (1986) applied the series solution to study the free vibration of free annular plates. So and Leissa (1998) used simple algebraic polynomials as admissible functions to calculate eigenfrequencies of thick, annular plates with free edges by the Ritz method, while Liew and Yang (1999, 2000) used orthogonally generated polynomials as admissible functions to analyze such plates with arbitrary edge conditions. Tzou et al. (1998) studied the in-plane modes of arbitrary thick disks by using the orthonormal polynomials and Legendre polynomials as admissible functions. Fan and Ye (1990) used the state-space method to investigate the free vibration of laminated circular plates. Liu and Lee (1997) used the finite element method to analyze the axisymmetric straining modes of circular plates.

Recently, the authors tried to use Chebyshev polynomials as admissible functions to study the three-dimensional vibrational characteristics of structural elements such as rectangular thick plates (Zhou et al., 2002a), triangular thick plates (Cheung and Zhou, 2002) and tori (Zhou et al., 2002b). In the present work, this is extended to study the vibration of thick, circular and annular plates with any boundary conditions, based on the three-dimensional, small strain elasticity theory. High accuracy and numerical reliability have been verified by the convergence study. In particular, due to the excellent property of Chebyshev polynomials in numerical operation, the present method can predict more eigenfrequencies with high accuracy compared with similar methods using some other polynomial functions.

2. Theoretical formulation

Consider an isotropic, thick, annular plate with outer radius R_1 and inner radius R_0 and thickness t as shown in Fig. 1. An orthogonal cylindrical coordinate system (r, θ, z) is defined with r in the radial direction, θ in the circumferential direction and z in the thickness direction. The corresponding displacement components at a generic point are u, v, and w in the r, θ and z direction, respectively.

The linear elastic strain energy V for an annular plate is given in integral form as

$$V = \frac{G}{2}\int_{R_0}^{R_1}\int_0^{2\pi}\int_{-t/2}^{t/2}\left(\frac{2v}{1-2v}(\varepsilon_{rr}+\varepsilon_{\theta\theta}+\varepsilon_{zz})^2 + 2(\varepsilon_{rr}^2+\varepsilon_{\theta\theta}^2+\varepsilon_{zz}^2)+\varepsilon_{r\theta}^2+\varepsilon_{rz}^2+\varepsilon_{\theta z}^2\right) r\,\mathrm{d}z\,\mathrm{d}\theta\,\mathrm{d}r, \tag{1}$$

where G is the shear modulus and v is the Poisson's ratio. The strain components ε_{ij} (i, $j = r$, θ, z) are defined as follows

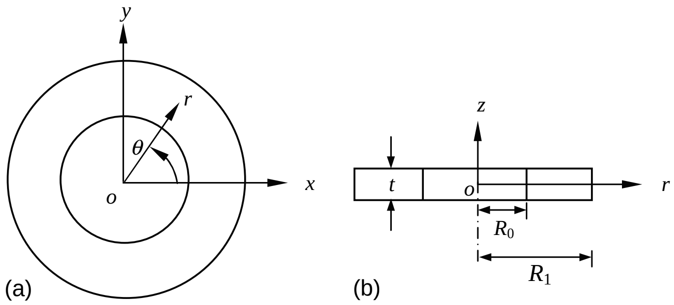

Fig. 1. Geometry, coordinates and dimensions of an annular plate: (a) the plan; (b) the cross-section.

$$\varepsilon_{rr}=\frac{\partial u}{\partial r};\quad \varepsilon_{\theta\theta}=\frac{u}{r}+\frac{\partial v}{r\partial\theta};\quad \varepsilon_{zz}=\frac{\partial w}{\partial z},$$
$$\varepsilon_{r\theta}=\frac{\partial u}{r\partial\theta}+\frac{\partial v}{\partial r}-\frac{v}{r};\quad \varepsilon_{rz}=\frac{\partial u}{\partial z}+\frac{\partial w}{\partial r};\quad \varepsilon_{\theta z}=\frac{\partial v}{\partial z}+\frac{\partial w}{r\partial\theta}. \tag{2}$$

The kinetic energy T of the plate can be given as

$$T=\frac{\rho}{2}\int_{R_0}^{R_1}\int_0^{2\pi}\int_{-t/2}^{t/2}\left(\left(\frac{\partial u}{\partial t}\right)^2+\left(\frac{\partial v}{\partial t}\right)^2+\left(\frac{\partial w}{\partial t}\right)^2\right)r\,\mathrm{d}z\,\mathrm{d}\theta\,\mathrm{d}r, \tag{3}$$

where ρ is the mass density per unit volume.

For simplicity and convenience in the mathematical formulation, the following dimensionless parameters are introduced

$$\bar{r}=\frac{2r}{\overline{R}}-\delta;\quad \bar{\theta}=\theta;\quad \bar{z}=\frac{2z}{t}, \tag{4}$$

where $\overline{R}=R_1-R_0$ and $\delta=(R_1+R_0)/(R_1-R_0)$. It is obvious that $R_0=0$, $\overline{R}=R_1$ and $\delta=1$ for a solid circular plate.

For free vibration analysis, the displacement components of the plate can be expressed in terms of the displacement amplitude functions as follows

$$u(r,\theta,z,t)=U(\bar{r},\bar{\theta},\bar{z})\mathrm{e}^{\mathrm{i}\omega t};\quad v(r,\theta,z,t)=V(\bar{r},\bar{\theta},\bar{z})\mathrm{e}^{\mathrm{i}\omega t};\quad w(r,\theta,z,t)=W(\bar{r},\bar{\theta},\bar{z})\mathrm{e}^{\mathrm{i}\omega t}, \tag{5}$$

where ω denotes the eigenfrequency of the plate and $\mathrm{i}=\sqrt{-1}$.

Considering the circumferential symmetry of the circular plate about the coordinate $\bar{\theta}$, the displacement amplitude functions can be expressed by

$$U(\bar{r},\bar{\theta},\bar{z})=\overline{U}(\bar{r},\bar{z})\cos(s\bar{\theta});\quad V(\bar{r},\bar{\theta},\bar{z})=\overline{V}(\bar{r},\bar{z})\sin(s\bar{\theta});\quad W(\bar{r},\bar{\theta},\bar{z})=\overline{W}(\bar{r},\bar{z})\cos(s\bar{\theta}), \tag{6}$$

where s is the circumferential wave number, which should be taken to be an integer (namely $s=0,1,2,\ldots,\infty$) to ensure the periodicity in the $\bar{\theta}$ direction. It is obvious that $s=0$ means the axisymmetric vibration. In such a case, $U(\bar{r},\bar{\theta},\bar{z})=\overline{U}(\bar{r},\bar{z})$; $V(\bar{r},\bar{\theta},\bar{z})=0$; $W(\bar{r},\bar{\theta},\bar{z})=\overline{W}(\bar{r},\bar{z})$. Rotating the symmetry axes by $\pi/2$, another set of free vibration modes can be obtained, corresponding to an interchange of

$\cos(s\theta)$ and $\sin(s\theta)$ in Eq. (6). However, in such a case, $s=0$ means $U(\bar{r},\bar{\theta},\bar{z})=0$; $V(\bar{r},\bar{\theta},\bar{z})=\overline{V}(\bar{r},\bar{z})$; $W(\bar{r},\bar{\theta},\bar{z})=0$, representing torsional vibration.

Substituting Eqs. (4)–(6) into Eqs. (1)–(3) gives the maximum potential energy $V_{\max}$ and kinetic energy $T_{\max}$ of the plate respectively as

$$V_{\max}=\frac{Gt}{2}\int_{-1}^{1}\int_{-1}^{1}\left(\frac{2v}{1-2v}\Gamma_1(\bar{\varepsilon}_{\bar{r}\bar{r}}+\bar{\varepsilon}_{\bar{\theta}\bar{\theta}}+\bar{\varepsilon}_{\bar{z}\bar{z}})^2 + 2\Gamma_1(\bar{\varepsilon}_{\bar{r}\bar{r}}^2+\bar{\varepsilon}_{\bar{\theta}\bar{\theta}}^2+\bar{\varepsilon}_{\bar{z}\bar{z}}^2)+\Gamma_2(\bar{\varepsilon}_{\bar{r}\bar{\theta}}^2+\bar{\varepsilon}_{\bar{r}\bar{z}}^2+\bar{\varepsilon}_{\bar{\theta}\bar{z}}^2)\right)(\bar{r}+\delta)\,\mathrm{d}\bar{z}\,\mathrm{d}\bar{r}; \tag{7}$$

$$T_{\max}=\frac{\rho\overline{R}^2t}{16}\omega^2\int_{-1}^{1}\int_{-1}^{1}(\Gamma_1\overline{U}^2+\Gamma_2\overline{V}^2+\Gamma_1\overline{W}^2)(\bar{r}+\delta)\,\mathrm{d}\bar{z}\,\mathrm{d}\bar{r}$$

in terms of the strains

$$\bar{\varepsilon}_{\bar{r}\bar{r}}=\frac{\partial\overline{U}}{\partial\bar{r}};\quad \bar{\varepsilon}_{\bar{\theta}\bar{\theta}}=\frac{\overline{U}}{\bar{r}+\delta}+\frac{s\overline{V}}{\bar{r}+\delta};\quad \bar{\varepsilon}_{\bar{z}\bar{z}}=\frac{\partial\overline{W}}{\bar{\gamma}\partial\bar{z}},$$
$$\bar{\varepsilon}_{\bar{r}\bar{\theta}}=-\frac{s\overline{U}}{\bar{r}+\delta}+\frac{\partial\overline{V}}{\partial\bar{r}}-\frac{\overline{V}}{\bar{r}+\delta};\quad \bar{\varepsilon}_{\bar{r}\bar{z}}=\frac{\partial\overline{U}}{\bar{\gamma}\partial\bar{z}}+\frac{\partial\overline{W}}{\partial\bar{r}};\quad \bar{\varepsilon}_{\bar{\theta}\bar{z}}=\frac{\partial\overline{V}}{\bar{\gamma}\partial\bar{z}}-\frac{s\overline{W}}{\bar{r}+\delta} \tag{8}$$

in which

$$\Gamma_1=\int_0^{2\pi}\cos^2(s\theta)\,\mathrm{d}\theta=\begin{cases}2\pi & \text{if } s=0,\\ \pi & \text{if } s>0,\end{cases}$$
$$\Gamma_2=\int_0^{2\pi}\sin^2(s\theta)\,\mathrm{d}\theta=\begin{cases}0 & \text{if } s=0,\\ \pi & \text{if } s>0,\end{cases}\quad \bar{\gamma}=t/\overline{R}. \tag{9}$$

Each of the displacement amplitude functions is written in the form of double series of Chebyshev polynomials multiplied by boundary functions as follows

$$\overline{U}(\bar{r},\bar{z})=F_u^0(\bar{r})F_u^1(\bar{r})\sum_{i=1}^{I}\sum_{j=1}^{J}A_{ij}P_i(\bar{r})P_j(\bar{z});$$
$$\overline{V}(\bar{r},\bar{z})=F_v^0(\bar{r})F_v^1(\bar{r})\sum_{k=1}^{K}\sum_{l=1}^{L}B_{kl}P_k(\bar{r})P_l(\bar{z}); \tag{10}$$
$$\overline{W}(\bar{r},\bar{z})=F_w^0(\bar{r})F_w^1(\bar{r})\sum_{m=1}^{M}\sum_{n=1}^{N}C_{mn}P_m(\bar{r})P_n(\bar{z}),$$

where I; J; K; L; M; N; are the truncation orders of the Chebyshev polynomial series and $A_{ij}B_{kl}C_{mn}$ are coefficients yet to be determined. $P_i(\chi)$ $(i=1,2,3,\ldots;\ \chi=\bar{r},\bar{z})$ is the one-dimensional sth Chebyshev polynomial which can be exactly written in terms of cosine functions as follows

$$P_i(\chi)=\cos[(i-1)\arccos(\chi)];\quad i=1,2,3,\ldots \tag{11}$$

The boundary functions $F_u^i(\bar{r})$; $F_v^i(\bar{r})$; $F_w^i(\bar{r})$ ($i=0$, 1) should enable the displacement components u; v; w to satisfy the inner and outer geometric boundary conditions of the plate, respectively. It is clear that $F_u^0(\bar{r})$; $F_v^0(\bar{r})$; $F_w^0(\bar{r})=1$ for a solid circular plate. The boundary functions corresponding to common boundary conditions are given in Table 1.

Table 1
Boundary functions for different boundary conditions

Boundary conditions	$F_u^0(\bar{r})$	$F_v^0(\bar{r})$	$F_w^0(\bar{r})$	$F_u^1(\bar{r})$	$F_v^1(\bar{r})$	$F_w^1(\bar{r})$
Clamped	$1+\bar{r}$	$1+\bar{r}$	$1+\bar{r}$	$1-\bar{r}$	$1-\bar{r}$	$1-\bar{r}$
Completely free	1	1	1	1	1	1
Hard simply-supported	1	$1+\bar{r}$	$1+\bar{r}$	1	$1-\bar{r}$	$1-\bar{r}$
Sliding	$1+\bar{r}$	1	1	$1-\bar{r}$	1	1
Soft simply-supported	1	1	$1+\bar{r}$	1	1	$1-\bar{r}$

It should be noted that Chebyshev polynomial series $P_i(\chi)$ $(i = 1, 2, 3, \ldots)$ is a set of complete and orthogonal series in the interval [−1, 1]. This therefore ensures that the double series $P_i(\chi)P_j(\chi)$ $(i, j = 1, 2, 3, \ldots)$ is also a complete and orthogonal set in the plate region. Excellent properties of Chebyshev polynomial series in the approximation of functions have been well known (Fox and Parker, 1968). Therefore, more rapid convergence and better stability in numerical operation than other polynomial series can be expected.

The energy functional of the plate is defined as follows

$$\Pi = V_{\max} - T_{\max}. \tag{12}$$

Minimizing the above functional with respect to the coefficients, i.e.

$$\frac{\partial \Pi}{\partial A_{ij}} = 0; \quad \frac{\partial \Pi}{\partial B_{kl}} = 0; \quad \frac{\partial \Pi}{\partial C_{mn}} = 0 \tag{13}$$

leads to the following eigenfrequency equation

$$\left[\begin{pmatrix} [K^{uu}] & [K^{uv}] & [K^{uw}] \\ & [K^{vv}] & [K^{vw}] \\ \text{Sym} & & [K^{ww}] \end{pmatrix} - \overline{\Omega}^2 \begin{pmatrix} [M^{uu}] & [0] & [0] \\ & [M^{vv}] & [0] \\ \text{Sym} & & [M^{ww}] \end{pmatrix}\right] \begin{Bmatrix} \{A\} \\ \{B\} \\ \{C\} \end{Bmatrix} = \begin{Bmatrix} \{0\} \\ \{0\} \\ \{0\} \end{Bmatrix}, \quad s \geqslant 1, \tag{14}$$

$$\left[\begin{pmatrix} [K^{uu}] & [K^{uw}] \\ \text{Sym} & [K^{ww}] \end{pmatrix} - \overline{\Omega}^2 \begin{pmatrix} [M^{uu}] & [0] \\ \text{Sym} & [M^{ww}] \end{pmatrix}\right] \begin{Bmatrix} \{A\} \\ \{C\} \end{Bmatrix} = \begin{Bmatrix} \{0\} \\ \{0\} \end{Bmatrix}, \quad s = 0 \text{ for axisymmetric mode}, \tag{15}$$

$$([K^{vv}] - \overline{\Omega}^2 [M^{vv}])\{B\} = \{0\}, \quad s = 0 \text{ for torsional mode} \tag{16}$$

in which $\overline{\Omega} = \omega \overline{R}\sqrt{\rho/G}$, $[K^{ij}]$ and $[M^{ij}]$ $(i, j = u, v, w)$ are the stiffness sub-matrices and the diagonal mass sub-matrices, respectively. The column vectors $\{A\}$, $\{B\}$ and $\{C\}$ are composed of the unknown coefficients as follows

$$\begin{aligned} \{A\} &= \{ A_{11} \ \cdots \ A_{1J} \ A_{21} \ \cdots \ A_{2J} \ \cdots \ A_{I1} \ \cdots \ A_{IJ} \}^{\mathrm{T}}; \\ \{B\} &= \{ B_{11} \ \cdots \ B_{1L} \ B_{21} \ \cdots \ B_{2L} \ \cdots \ B_{K1} \ \cdots \ B_{KL} \}^{\mathrm{T}}; \\ \{C\} &= \{ C_{11} \ \cdots \ C_{1N} \ C_{21} \ \cdots \ C_{2N} \ \cdots \ C_{M1} \ \cdots \ C_{MN} \}^{\mathrm{T}}. \end{aligned} \tag{17}$$

The elements of the sub-matrices $[K^{ij}]$ and $[M^{ij}]$ $(i,j=u,v,w)$ are given by

$$\begin{aligned}
[K^{uu}] &= \frac{1-v}{1-2v}(D^{111}_{uiu\bar{i}}+D^{00-1}_{uiu\bar{i}})H^{00}_{uju\bar{j}}+\frac{v}{1-2v}(D^{010}_{uiu\bar{i}}+D^{100}_{uiu\bar{i}})H^{00}_{uju\bar{j}}\\
&\quad+\frac{1}{2\bar{\gamma}^2}(s^2\bar{\gamma}^2D^{00-1}_{uiu\bar{i}}H^{00}_{uju\bar{j}}+D^{001}_{uiu\bar{i}}H^{11}_{uju\bar{j}});\\
[K^{uv}] &= \frac{(1-v)s}{1-2v}D^{00-1}_{uiv\bar{k}}H^{00}_{ujv\bar{l}}+\frac{vs}{1-2v}D^{100}_{uiv\bar{k}}H^{00}_{ujv\bar{l}}+\frac{s}{2}(D^{00-1}_{uiv\bar{k}}-D^{010}_{uiv\bar{k}})H^{00}_{ujv\bar{l}};\\
[K^{uw}] &= \frac{v}{(1-2v)\bar{\gamma}}(D^{101}_{uiw\bar{m}}+D^{000}_{uiw\bar{m}})H^{01}_{ujw\bar{n}}+\frac{1}{2\bar{\gamma}}D^{011}_{uiw\bar{m}}H^{10}_{ujw\bar{n}};\\
[K^{vv}] &= \frac{(1-v)s^2}{1-2v}D^{00-1}_{vkv\bar{k}}H^{00}_{vlv\bar{l}}+\frac{1}{2}(D^{111}_{vkv\bar{k}}+D^{00-1}_{vkv\bar{k}}-D^{010}_{vkv\bar{k}}-D^{100}_{vkv\bar{k}})H^{00}_{vlv\bar{l}}+\frac{1}{2\bar{\gamma}^2}D^{001}_{vkv\bar{k}}H^{11}_{vlv\bar{l}};\\
[K^{vw}] &= \frac{vs}{(1-2v)\bar{\gamma}}D^{000}_{vkw\bar{m}}H^{01}_{vlw\bar{n}}+\frac{s}{2\bar{\gamma}}D^{000}_{vkw\bar{m}}H^{10}_{vlw\bar{n}};\\
[K^{ww}] &= \frac{1-v}{(1-2v)\bar{\gamma}^2}D^{001}_{wmw\bar{m}}H^{11}_{wnw\bar{n}}+\frac{1}{2}(D^{111}_{wmw\bar{m}}+s^2D^{00-1}_{wmw\bar{m}})H^{00}_{wnw\bar{n}};\\
[M^{uu}] &= D^{001}_{uiu\bar{i}}H^{00}_{uju\bar{j}}/8;\quad [M^{vv}]=D^{001}_{vkv\bar{k}}H^{00}_{vlv\bar{l}}/8;\\
[M^{ww}] &= D^{001}_{wmw\bar{m}}H^{00}_{wnw\bar{n}}/8
\end{aligned} \tag{18}$$

in which

$$\begin{aligned}
D^{abc}_{\alpha\sigma\beta\tau} &= \int_{-1}^{1}\frac{\mathrm{d}^a[F_\alpha(\bar{r})P_\sigma(\bar{r})]}{\mathrm{d}\bar{r}^a}\frac{\mathrm{d}^b[F_\beta(\bar{r})P_\tau(\bar{r})]}{\mathrm{d}\bar{r}^b}(\bar{r}+\delta)^c\,\mathrm{d}\bar{r};\\
H^{ab}_{\alpha\sigma\beta\tau} &= \int_{-1}^{1}\frac{\mathrm{d}^aP_\sigma(\bar{z})}{\mathrm{d}\bar{z}^a}\frac{\mathrm{d}^bP_\tau(\bar{z})}{\mathrm{d}\bar{z}^b}\,\mathrm{d}\bar{z},\quad a;b=0;1,\ \ c=0;1;-1,\\
\alpha;\beta &= u;v;w,\quad \sigma=i;k;m;j;l;n,\quad \tau=\bar{i};\bar{k};\bar{m};\bar{j};\bar{l};\bar{n},
\end{aligned} \tag{19}$$

where $F_\alpha(\bar{r})=F^0_\alpha(\bar{r})F^1_\alpha(\bar{r})$ and $F_\beta(\bar{r})=F^0_\beta(\bar{r})F^1_\beta(\bar{r})$.

A non-trivial solution is obtained by setting the determinant of the coefficient matrix of Eqs. (14)–(16) equal to zero, respectively. Roots of the determinant are the square of the eigenvalues (dimensionless eigenfrequency) $\overline{\Omega}$. Eigenfunctions, i.e. mode shapes, corresponding to the eigenvalues are determined by back-substitution of the eigenvalues, one by one, in the usual manner.

3. Convergence and comparison study

Before accepting a strategy for approximate solution, it is very important to check its accuracy, convergence and numerical stability. Firstly, a convergence study is performed for a clamped–clamped annular plate with inner–outer radius ratio $R_1/R_0=2.5$, thickness–radius ratio $\gamma=t/R_1=0.5$. In the following study, Poisson's ratio is taken as $v=0.3$. For simplicity, equal numbers of Chebyshev polynomial terms were taken for each of the displacement amplitude functions $\overline{U}$, $\overline{V}$ and $\overline{W}$ in each coordinate direction, namely $I=K=M$ and $J=L=N$, although in most cases, using unequal numbers of series terms may be more efficient in computation. In all the following computations, double precision (16 significant figures) computation is used and the zero eigenfrequencies (rigid body modes) are excluded from the results. Table 2

Table 2
Convergence of the first eight eigenfrequency parameters for various vibration categories of a clamped–clamped annular plate with inner–outer radius ratio $R_1/R_0 = 2.5$ and thickness–radius ratio $\gamma = t/R_1 = 0.5$

s	$I \times J$	Ω_1	Ω_2	Ω_3	Ω_4	Ω_5	Ω_6	Ω_7	Ω_8
Antisymmetric modes in the thickness direction									
0^a	9×4	4.663	8.952	11.40	14.35	17.29	19.23	19.49	21.88
	12×7	4.660	8.950	11.40	14.34	17.28	19.22	19.48	21.87
	20×15	4.660	8.950	11.40	14.34	17.28	19.22	19.48	21.87
0^t	9×4	8.279	12.29	16.97	19.61	21.61	21.91	24.58	26.98
	11×5	8.279	12.29	16.97	19.61	21.60	21.91	24.57	26.96
	20×15	8.279	12.29	16.97	19.61	21.60	21.91	24.57	26.96
1	9×4	4.753	8.536	9.127	11.23	12.74	14.42	16.75	17.64
	15×9	4.750	8.536	9.126	11.23	12.74	14.42	16.75	17.64
	20×15	4.750	8.536	9.126	11.23	12.74	14.42	16.75	17.64
2	9×4	5.091	9.097	9.710	11.15	13.65	14.65	16.56	18.19
	15×8	5.088	9.096	9.708	11.15	13.65	14.65	16.56	18.18
	20×15	5.088	9.096	9.708	11.15	13.65	14.65	16.56	18.18
3	9×4	5.724	9.745	10.58	11.43	14.74	15.03	16.55	18.76
	11×7	5.722	9.744	10.58	11.43	14.73	15.02	16.55	18.76
	20×15	5.722	9.744	10.58	11.43	14.73	15.02	16.55	18.76
Symmetric modes in the thickness direction									
0^a	9×4	9.124	11.63	12.65	15.64	16.52	19.08	20.37	22.19
	16×9	9.117	11.63	12.65	15.62	16.52	19.08	20.34	22.18
	20×15	9.117	11.63	12.65	15.62	16.52	19.08	20.34	22.18
0^t	8×3	5.391	10.56	13.72	15.77	16.45	20.19	20.99	24.49
	9×4	5.391	10.56	13.67	15.77	16.41	20.16	20.99	24.46
	20×15	5.391	10.56	13.67	15.77	16.41	20.16	20.99	24.46
1	9×4	5.798	9.005	10.86	11.58	12.84	13.95	15.70	15.81
	12×9	5.798	9.000	10.86	11.58	12.84	13.95	15.69	15.82
	20×15	5.798	9.000	10.86	11.58	12.84	13.95	15.69	15.81
2	9×4	6.786	8.994	11.15	11.81	13.51	14.52	15.71	15.94
	16×9	6.785	8.991	11.15	11.80	13.51	14.52	15.71	15.94
	20×15	6.785	8.991	11.15	11.80	13.51	14.52	15.71	15.94
3	9×4	7.903	9.374	11.34	12.30	14.55	15.18	15.76	16.24
	13×8	7.901	9.372	11.34	12.30	14.55	15.18	15.76	16.24
	20×15	7.901	9.372	11.34	12.30	14.55	15.18	15.76	16.24

Note: 0^a means axisymmetric mode. 0^t means torsional mode.

shows the convergence of the first eight eigenfrequency parameters for different modes. Ten types of vibration modes are considered. They are symmetric and antisymmetric modes for axisymmetric vibration ($s = 0^a$), symmetric and antisymmetric modes for torsional vibration ($s = 0^t$), and symmetric and antisymmetric modes for circumferential vibrations for wave number $s = 1$, 2, 3. Another dimensionless eigenfrequency parameter $\Omega = \omega R_1 \sqrt{\rho/G}$ was adopted for convenience in expression and comparison. All results converged to at least four significant figures. It is seen that the fastest convergence is obtained for the symmetric mode of torsional vibration. In such a case, 9 terms in the radial direction and 4 terms in the thickness direction (i.e. 9×4 terms) are needed only. The slowest convergence is observed for the symmetric mode of circumferential vibrations for wave number $s = 2$. In such a case, 16×9 terms are necessary. It should be mentioned that among various boundary conditions, the clamped condition is the slowest in convergence in the Ritz method because of the stress singularities which occur in the corner at the fixed ends. For plates with other boundary conditions, more rapid convergence could be expected.

It is well known that in the Ritz method, to obtain more accurate results and/or more number of eigenfrequencies, normally more terms of admissible functions have to be used. However, sometimes this will result in an ill-conditioned eigenvalue problem. The occurrence of ill-conditioning sooner or later with the increase in number of terms used is greatly dependent on the kind of admissible functions adopted in the analysis, apart from the precision of numerical computation used. In a recent paper, So and Leissa (1998) used simple algebraic polynomials as the admissible functions to study the free vibration of solid circular

Table 3
Convergence of the first five lower-order and three higher-order eigenfrequency parameters for various vibration categories of a completely free solid circular plate with thickness–radius ratio $\gamma = 0.4$

s	$I \times J$	Ω_1	Ω_2	Ω_3	Ω_4	Ω_5	Ω_{10}	Ω_{20}	Ω_{30}
Antisymmetric modes in the thickness direction									
0^a	10×4	1.4640	4.4150	7.3529	9.3232	11.093	19.015	29.719	42.065
	20×10	1.4640	4.4150	7.3529	9.3230	11.088	19.013	26.911	33.249
	30×15	1.4640	4.4150	7.3529	9.3230	11.088	19.013	26.910	33.241
0^t	10×4	7.8540	9.3840	11.512	14.026	16.792	25.078	43.111	116.10
	20×10	7.8540	9.3840	11.512	14.025	16.751	25.020	36.153	43.182
	30×15	7.8540	9.3840	11.512	14.025	16.751	25.020	36.153	43.182
1	10×4	2.7796	5.8443	8.0376	8.2965	9.1687	14.058	23.509	28.590
	20×10	2.7796	5.8443	8.0376	8.2965	9.1685	14.026	22.729	26.902
	30×15	2.7796	5.8443	8.0376	8.2965	9.1685	14.026	22.729	26.902
2	10×4	0.9078	4.0893	7.0875	8.8811	8/9843	14.318	23.952	29.725
	20×10	0.9078	4.0893	7.0875	8.8811	8.9843	14.275	23.430	26.830
	30×15	0.9078	4.0893	7.0875	8.8811	8.9843	14.275	23.430	26.830
3	10×4	1.8600	5.3530	8.1546	9.7233	10.069	15.827	24.772	31.248
	20×10	1.8600	5.3530	8.1546	9.7232	10.069	15.674	23.827	28.169
	30×15	1.8600	5.3530	8.1546	9.7232	10.069	15.674	23.827	28.167
Symmetric modes in the thickness direction									
0^a	10×5	3.4364	8.5887	11.488	11.610	13.384	17.588	31.123	44.014
	20×10	3.4364	8.5887	11.488	11.610	13.383	17.425	28.652	34.413
	30×15	3.4364	8.5887	11.488	11.610	13.383	17.425	28.648	34.411
0^t	10×5	5.1356	8.4172	11.620	14.842	15.708	21.611	35.634	91.043
	20×10	5.1356	8.4172	11.620	14.796	15.708	21.117	31.833	39.699
	30×15	5.1356	8.4172	11.620	14.796	15.708	21.117	31.833	39.699
1	10×5	2.7308	5.8639	6.8123	9.9032	10.366	14.473	20.483	27.940
	20×10	2.7308	5.8639	6.8123	9.9032	10.366	14.467	19.521	25.258
	30×15	2.7308	5.8639	6.8123	9.9032	10.366	14.467	19.521	25.258
2	10×5	2.3455	4.2296	7.5012	8.5599	11.122	14.677	21.067	29.639
	20×10	2.3455	4.2296	7.5012	8.5599	11.122	14.643	20.830	26.270
	30×15	2.3455	4.2296	7.5012	8.5599	11.122	14.643	20.830	26.270
3	10×5	3.6000	5.7935	8.8324	10.105	11.611	16.080	22.477	31.264
	20×10	3.6000	5.7935	8.8324	10.105	11.611	16.042	22.354	27.483
	30×15	3.6000	5.7935	8.8324	10.105	11.611	16.042	22.354	27.483

Note: 0^a means axisymmetric mode. 0^t means torsional mode.

and annular thick plates with completely free edges, and the first five eigenfrequency parameters with rather high accuracy have been obtained. However, they also reported that ill-conditioning occurred for a solid circular plate with thickness–radius ratio $\gamma = 0.4$ if more than 10×4 terms were used. This limit on the polynomial orders means that only several eigenfrequencies of lower order can be obtained with satisfactory accuracy. The present analysis shows that with the increase of plate thickness, the eigenfrequencies tend to huddle together. In some cases, a large number of vibration modes are required. For example, when a thick plate is acted upon by a shock load with a wide spectrum, only a large number of vibration modes can provide a realistic dynamic response. Using Chebyshev polynomials as the admissible functions, the immunity against ill-conditioned behaviour can be greatly enhanced. Table 3 gives the convergence of the first five lower-order (Ω_1–Ω_5) and three higher-order (Ω_{10}, Ω_{20}, Ω_{30}) eigenfrequency parameters for various vibration categories of a completely free solid circular plate with thickness–radius ratio $\gamma = 0.4$. It is shown that if only 10×4 terms are used, the accuracy of the higher-order eigenfreuqency parameters $\overline{\Omega}_{20}$ and $\overline{\Omega}_{30}$ is not satisfactory. However, if 20×10 terms are used, highly accurate results can be obtained. This has also been demonstrated by the results obtained by using 30×15 terms, and it should be mentioned that it has not reached the upper limit yet. The authors have indeed tried to use 50×25 terms, and stable numerical operation can still be carried out.

A comparison study has been given in Table 4 for solid and annular circular plates with different boundary conditions. For simplicity in comparison, a new dimensionless eigenfrequency parameter $\Lambda = \omega R_1^2 (\rho t/D)^{1/2}$ was used where D is the flexural stiffness and all the eigenfrequencies are listed only in order of magnitude but not their vibration categories. The results in parentheses are taken from Liew and

Table 4
Comparison of the present solutions with the orthogonal generated polynomial solutions by Liew and Yang (1999, 2000)

$\gamma = t/R$	Λ_1	Λ_2	Λ_3	Λ_4	Λ_5	Λ_6	Λ_7	Λ_8
Completely free solid circular plates								
0.1	5.2791	8.8720**	12.072	19.737	20.826	31.327	33.110	36.132**
	(5.2795)	(8.8720)	(12.074)	(19.738)	(20.831)	(31.336)	(33.112)	(36.132)
0.3	4.9005	8.0344**	10.439	16.023	16.102	16.750	18.666	23.503
	(4.9005)	(8.0344)	(10.439)	(16.023)	(16.102)	(16.750)	(18.666)	(23.503)
0.5	4.3913	6.9727**	8.6854	9.6135	11.185	12.578	13.145	14.018**
	(4.3913)	(6.9727)	(8.6854)	(9.6135)	(11.185)	(12.578)	(13.145)	(14.018)
Clamped solid circular plates								
0.1	9.9755**	20.267	32.383	36.692**	46.076	54.234	61.113	67.941
	(9.9909)	(20.297)	(32.430)	(36.744)	(46.140)	(54.308)	(61.186)	(67.969)
0.3	8.4606**	15.442	22.654	22.715	25.134**	26.176*	30.078	34.222
	(8.4676)	(15.453)	(22.667)	(22.721)	(25.150)	–	(30.093)	(34.239)
0.5	6.8027**	11.492	13.654	15.705*	16.224	17.819**	21.024	21.183
	(6.8068)	(11.497)	(13.658)	–	(16.229)	(17.825)	(21.029)	(21.188)
Annular plate with clamped inner edge and free outer edge, $R_1/R_0 = 10/3$								
0.2	5.8498	6.1864**	6.9366	9.7590*	11.756	18.832	18.972	27.409
	[5.8662]	[6.2020]	[6.9482]	–	[11.769]	[18.833]	[18.973]	–
Annular plate with free inner edge and clamped outer edge, $R_1/R_0 = 10/3$								
0.2	10.437**	16.012	25.632	36.194	37.309**	39.591	40.534*	44.066
	[10.448]	[16.026]	[25.650]	[36.220]	[37.346]	[39.602]	–	–
Annular plate with both edges clamped, $R_1/R_0 = 10/3$								
0.2	30.688**	31.422	34.325	40.231	48.220*	48.707	53.067	58.689
	[30.743]	[31.474]	[34.370]	[40.266]	–	[48.736]	[53.072]	–

Notes: 1. *Eigenfrequencies of the torsional vibration; **eigenfrequencies of the axisymmetric vibration. 2. Data in parentheses are taken from Liew and Yang (1999). 3. Data in square brackets are taken from Liew and Yang (2000).

Yang (1999) while those in square brackets are taken from Liew and Yang (2000), using the orthogonal generated polynomials. Apart from those of the torsional vibration which are not given by Liew and Yang, good agreement has been achieved. However, some obvious difference between the present eigenfrequencies and those of Liew and Yang for circular plates with one or both edges clamped can be observed. It is seen that for both solid and annular circular plates with clamped edges, the present results are all lower than those of Liew and Yang. Since these solutions all converge from above, this would indicate the higher accuracy of the present solutions. Table 5 re-examines the discrepancies between the Rayleigh–Ritz solutions of So and Leissa (1998) and the series solutions of Hutchinson and El-Azhari (1986). It is observed that the present solutions are essentially the same as those of So and Leissa and, in most cases, agree with those of Hutchinson and El-Azhari. However, some obvious disagreement can be observed. For examples, in the results of Hutchinson and El-Azhari, the fourth eigenfrequency parameter 10.398 for $t/R_1 = 0.4$ and $s = 0^a$, the third and fourth eigenfrequency parameters 7.503 and 8.259 respectively for $t/R_1 = 1$ and $s = 0^a$, and the fourth eigenfrequency parameter 6.401 for $t/R_1 = 1$ and $s = 1$ are much lower than the others. The eigenfrequency parameters from the present solution are 14.133, 8.258, 9.084 and 7.706, respectively. On the other hand, from the results of Hutchinson and El-Azhari, the third and fourth eigenfrequency parameters 8.990 and 10.234 respectively for $t/R_1 = 0.4$ and $s = 3$ are much higher than the others, and the present results are 8.808 and 8.986, respectively. Moreover, in the results of Hutchinson and El-Azhari, the

Table 5
Comparison of the first four eigenfrequency parameters for antisymmetric modes of completely free annular plates with inner–outer radius ratio $R_1/R_0 = 2$ when circumferential wave numbers $s = 0^a$, 1, 2, 3

t/R_1	s	Method	Ω_1	Ω_2	Ω_3	Ω_4
0.4	0^a	Present	1.388	8.321	9.127	14.133
		So and Leissa (1998)	1.388	8.321	9.127	14.133
		Hutchinson and El-Azhari (1986)	1.398	8.327	9.128	**10.398**
	1	Present	1.943	8.039	8.534	8.945
		So and Leissa (1998)	1.943	8.039	8.534	8.945
		Hutchinson and El-Azhari (1986)	1.950	8.040	8.539	8.946
	2	Present	0.691	3.123	8.400	8.793
		So and Leissa (1998)	0.691	3.123	8.400	8.793
		Hutchinson and El-Azhari (1986)	**6.901**	3.127	8.404	8.794
	3	Present	1.680	4.450	8.808	8.986
		So and Leissa (1998)	1.680	4.450	8.808	8.986
		Hutchinson and El-Azhari (1986)	1.682	4.453	**8.990**	**10.234**
1	0^a	Present	1.984	5.772	8.258	9.084
		So and Leissa (1998)	1.984	5.772	8.258	9.084
		Hutchinson and El-Azhari (1986)	1.985	5.774	**7.503**	**8.259**
	1	Present	1.999	3.930	5.839	7.706
		So and Leissa (1998)	1.999	3.930	5.839	7.706
		Hutchinson and El-Azhari (1986)	2.000	3.930	5.841	**6.401**
	2	Present	1.039	2.846	5.172	6.157
		So and Leissa (1998)	1.039	2.846	5.172	6.157
		Hutchinson and El-Azhari (1986)	1.040	2.846	5.173	6.159
	3	Present	2.320	3.946	6.392	6.805
		So and Leissa (1998)	2.320	3.946	6.392	6.805
		Hutchinson and El-Azhari (1986)	2.321	3.946	6.392	6.806

Table 6
Comparison of the present solutions with those of the classical plate theory by Leissa (1969) for a thin solid circular plate with thickness–radius ratio $\gamma = t/R = 0.01$

s	Λ_1	Λ_2	Λ_3	Λ_4	Λ_5	Λ_6	Λ_7	Λ_8
Completely free solid circular plate								
0	9.0766	38.519	87.761	156.59	244.85	352.35	478.86	624.13
	(9.084)	(38.55)	(87.80)	(157.0)	(245.9)	(354.6)	(483.1)	(631.0)
1	20.521	59.848	118.86	197.41	295.30	412.33	548.24	702.78
	(20.52)	(59.86)	(119.0)	(198.2)	(296.9)	(415.3)	(651.8)	(711.3)
2	5.2634	35.233	84.305	153.03	241.22	348.68	475.17	620.42
	(5.253)	(35.25)	(83.9)	(154.0)	(242.7)	(350.8)	(479.2)	(627.0)
3	12.240	52.873	111.73	190.15	287.95	404.93	540.82	695.35
	(12.23)	(52.91)	(111.3)	(192.1)	(290.7)	(408.4)	(546.2)	(703.3)
Clamped solid circular plate								
0	10.226	39.785	89.046	157.87	246.10	353.56	480.01	625.19
	(10.216)	(39.771)	(89.104)	(158.18)	(247.01)	(355.57)	(483.87)	(631.91)
1	21.276	60.823	119.93	198.50	296.39	413.39	549.25	703.71
	(21.26)	(60.82)	(120.08)	(199.06)	(297.77)	(416.20)	(554.37)	(712.30)
2	34.892	84.534	153.52	241.85	349.37	475.88	621.11	784.79
	(34.88)	(84.58)	(153.81)	(242.71)	(351.38)	(479.65)	(627.75)	(795.52)
3	51.033	110.90	189.81	287.89	405.03	541.00	695.56	868.41
	(51.04)	(111.01)	(190.30)	(289.17)	(407.72)	(545.97)	(703.95)	(881.67)

Note: Data in parentheses are taken from Leissa (1969) and for the completely free plate, Poisson's ratio $\nu = 0.33$ was used while for the clamped plate, Poisson's ratio $\nu = 0.3$ was used.

first eigenfrequency parameter 6.901 for $t/R_1 = 0.4$ and $s = 2$ is an obvious typographic error as it should be lower than the second eigenfrequency parameter 3.127.

Table 6 compares the present solutions with those obtained from the classical 2D plate theory for thin plates. The first eight eigenfrequency parameters of antisymmetric modes for the clamped and completely free solid circular plate for wave number $s = 0$, 1, 2, 3, respectively, are considered. The plate has a thickness–radius ratio $\gamma = t/R = 0.01$. It is shown that the present results for thin plates are completely consistent with the classical solutions.

4. Numerical results

Most of the available three-dimensional elasticity solutions for free vibrations of circular and annular plates are for completely free plates (Hutchinson, 1979, 1984; Hutchinson and El-Azhari, 1986; So and Leissa, 1998). However, the results for circular and annular plates with other boundary conditions are very limited (Liew and Yang, 2000). In the following study, based on the convergence study shown in Tables 2 and 3, and the comparison shown in Tables 4–6, some numerical results are given for circular and annular plates with clamped inner and/or outer edges. In Tables 7 and 8, the first 30 eigenfrequency parameters Ω_i ($i = 1, 2, \ldots, 30$) of antisymmetric and symmetric modes of each of the vibration categories ($s = 0^a$, 0^t, 1, 2, 3) for an annular circular plate with free inner edge and clamped outer edge and both edges clamped are given, respectively. The plate has an inner–outer radius ratio $R_1/R_0 = 5.0$ and a thickness–radius ratio $\gamma = t/R_1 = 0.5$. The results are obtained by using 20×15 terms of the Chebyshev polynomials. From the tables, it can be seen that for the same order, the eigenfrequencies in Table 8 are always higher than the corresponding eigenfrequencies in Table 7 because of the more restrictive boundary conditions. Moreover,

Table 7
The first 30 eigenfrequency parameters Ω_i ($i = 1, 2, \ldots, 30$) of each of the vibration categories for an annular circular plate with free inner edge and clamped outer edge, inner–outer radius ratio $R_1/R_0 = 5.0$ and thickness–radius ratio $\gamma = t/R_1 = 0.5$

i	Antisymmetric modes					Symmetric modes				
	$s = 0^a$	$s = 0^t$	$s = 1$	$s = 2$	$s = 3$	$s = 0^a$	$s = 0^t$	$s = 1$	$s = 2$	$s = 3$
1	1.729	7.375	2.647	3.861	5.095	5.574	3.861	3.581	4.335	6.246
2	4.552	9.585	5.042	6.620	8.246	9.584	7.238	5.575	6.646	8.103
3	8.106	12.49	7.388	7.722	8.909	9.986	10.80	8.503	9.061	9.694
4	8.852	15.80	8.158	9.000	10.28	11.75	13.15	9.287	9.911	10.80
5	12.10	19.24	8.961	9.888	11.31	12.51	14.50	10.15	10.84	11.50
6	12.59	19.33	10.77	11.36	11.94	13.09	14.50	11.51	12.16	13.01
7	15.74	20.19	11.61	12.55	14.00	15.41	16.57	11.78	12.45	13.86
8	16.29	21.72	12.55	13.23	14.38	15.92	18.28	12.41	13.13	14.01
9	17.86	22.98	13.76	14.74	15.23	18.15	19.19	13.14	13.59	14.76
10	19.05	23.78	15.56	15.99	17.02	18.58	22.10	13.85	14.48	15.25
11	19.49	26.25	15.93	16.51	17.47	19.73	22.18	14.44	14.86	15.64
12	20.12	26.71	16.86	17.83	18.66	21.78	25.42	15.06	15.85	16.55
13	21.54	29.05	18.04	18.40	19.07	23.01	25.43	15.71	16.63	17.69
14	22.38	30.48	18.81	18.76	19.31	23.17	25.96	16.22	17.11	17.91
15	23.20	31.65	19.26	19.49	19.92	24.85	26.15	17.01	18.00	18.79
16	23.67	32.08	19.51	19.73	20.28	25.78	27.35	17.92	18.35	19.63
17	25.21	32.24	19.89	20.32	20.80	26.37	28.84	18.57	18.78	19.92
18	25.49	33.22	20.10	20.64	21.27	26.64	29.01	19.05	20.26	20.98
19	26.10	34.29	20.39	21.10	22.13	27.14	29.83	19.76	20.34	21.30
20	26.79	34.60	21.59	21.78	22.16	28.33	31.08	19.90	20.98	21.89
21	28.04	35.28	21.76	22.08	22.85	29.29	32.37	21.76	22.06	23.11
22	28.63	36.35	22.47	22.65	23.21	30.12	33.47	22.18	22.55	23.56
23	29.55	38.13	23.25	23.65	24.16	31.65	33.71	22.55	23.41	24.16
24	30.22	38.41	23.39	24.00	24.64	31.95	35.98	23.22	23.78	24.74
25	31.23	38.62	23.75	24.43	25.41	32.66	36.13	23.38	24.01	25.96
26	31.72	40.75	24.32	25.03	25.72	33.60	37.60	24.89	25.08	25.46
27	31.98	41.98	25.36	25.67	26.17	34.25	37.90	25.46	25.62	25.95
28	32.27	42.06	25.68	25.92	26.62	35.02	38.39	25.57	25.81	26.24
29	33.39	43.32	25.89	26.43	27.29	35.85	39.00	25.81	26.04	26.42
30	33.73	44.15	26.69	27.12	27.66	35.97	39.22	25.92	26.15	27.01

with the increase in order, the eigenfrequencies tend to huddle together while the smallest eigenfrequency is the fundamental one of antisymmetric mode.

The fundamental dimensionless eigenfrequency parameters $\Omega = \omega R_1\sqrt{\rho/G}$ of antisymmetric and symmetric modes for each of the vibration categories ($s = 0^a$, 0^t, 1, 2, 3) of annular plates with the clamped inner edge and free outer edge are then studied in detail. Five different outer–inner radius ratios $R_1/R_0 = 10, 10/3, 2, 10/7$ and 10/9 are considered. Figs. 2–6 plot the fundamental eigenfrequency parameters of each vibration category with respect to the thickness–radius ratio $\gamma = t/R_1$ ranging from 0.1 to 0.5 with an increment of 0.05. These results are obtained by using 13×7 terms of the Chebyshev polynomials and the Poisson's ratio is taken as $\nu = 0.3$.

Fig. 2 presents the fundamental eigenfrequency parameters of the antisymmetric and symmetric modes for torsional vibration. It is seen that for the antisymmetric mode, the eigenfrequencies monotonically decrease with the increase of thickness–radius ratio. While for the symmetric mode, the thickness–radius ratio has no effect on the fundamental eigenfrequencies for arbitrary outer–inner ratios. It is seen that when the outer–inner radius ratio decreases, both the eigenfrequencies of the antisymmetric and symmetric modes monotonically increase. In particular, when the outer–inner radius ratio R_1/R_0 is close to 1, such as those values below 10/7, the rapid increase of eigenfrequencies has been observed. Moreover, for the

Table 8
The first 30 eigenfrequency parameters Ω_i ($i = 1, 2, \ldots, 30$) of each of the vibration categories for an annular circular plate with both inner and outer edges clamped, inner–outer radius ratio $R_1/R_0 = 5.0$ and thickness–radius ratio $\gamma = t/R_1 = 0.5$

i	Antisymmetric modes					Symmetric modes				
	$s = 0^a$	$s = 0^t$	$s = 1$	$s = 2$	$s = 3$	$s = 0^a$	$s = 0^t$	$s = 1$	$s = 2$	$s = 3$
1	3.274	7.578	3.472	4.144	5.165	7.142	4.236	4.720	5.731	6.872
2	6.507	10.22	6.741	7.446	8.479	10.81	8.055	6.873	7.333	8.455
3	9.724	13.48	7.956	8.691	9.469	11.45	11.93	8.965	9.898	10.40
4	10.43	17.02	9.395	9.692	10.66	12.97	13.26	10.72	10.90	11.50
5	14.33	19.32	10.62	11.19	12.06	14.53	14.93	11.55	11.79	12.31
6	14.36	20.50	11.17	12.59	13.54	15.14	15.82	12.15	12.86	13.50
7	18.02	20.70	13.26	13.25	14.14	16.52	17.33	12.76	13.18	14.62
8	18.08	22.31	14.48	14.91	15.60	18.12	19.73	13.81	14.22	14.65
9	19.33	24.46	14.95	15.99	16.96	20.25	20.20	14.42	14.89	15.72
10	20.17	24.61	16.97	17.03	17.43	20.95	23.39	15.23	15.61	16.24
11	21.47	27.28	18.20	18.54	19.10	21.94	23.64	15.39	15.94	16.66
12	21.74	28.26	18.31	18.95	19.33	24.38	25.49	16.22	17.01	17.52
13	23.53	30.23	19.24	19.23	19.86	25.04	26.39	16.86	17.68	18.94
14	24.05	31.70	19.49	19.82	20.27	25.55	26.77	17.38	18.12	19.28
15	24.25	32.10	20.13	20.20	20.50	25.71	27.56	18.38	18.95	19.71
16	25.45	32.43	20.50	20.62	21.00	26.97	27.82	19.73	19.95	20.58
17	26.70	33.39	20.99	21.66	22.13	28.10	29.70	20.09	20.20	20.69
18	27.09	33.60	21.56	21.86	22.58	28.96	30.29	20.72	21.68	22.88
19	28.39	35.17	21.83	22.11	22.78	29.72	31.47	21.32	22.12	22.90
20	29.12	35.95	22.45	22.87	23.58	29.94	31.95	22.05	22.38	23.03
21	29.82	36.69	23.57	23.75	24.10	31.22	33.89	23.42	23.58	24.02
22	30.44	37.10	24.06	24.15	24.44	32.45	34.50	23.64	23.83	24.32
23	31.79	39.32	24.33	24.70	25.23	33.80	35.40	24.76	25.46	25.68
24	32.33	39.82	24.72	25.44	26.27	33.94	37.30	25.18	25.64	26.21
25	32.60	40.10	25.02	25.84	26.41	35.30	37.56	25.46	25.69	26.32
26	33.07	41.79	25.55	25.84	26.83	35.53	37.94	25.70	25.98	26.55
27	33.36	43.60	26.84	27.09	27.39	36.32	38.55	25.81	26.10	26.71
28	33.84	43.69	27.03	27.27	27.86	36.60	39.32	26.43	26.60	27.05
29	35.42	44.19	27.47	27.75	28.16	36.91	39.54	26.79	26.93	27.29
30	35.48	44.47	28.28	28.73	29.50	38.34	40.28	27.09	27.39	27.80

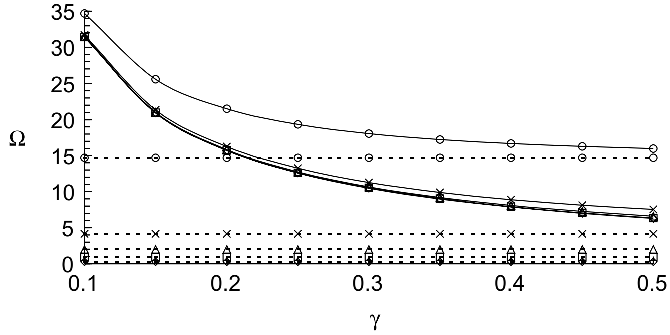

Fig. 2. The fundamental eigenfrequency parameters of torsional vibration ($s = 0^t$) for annular plates with clamped inner edge and free outer edge: antisymmetric modes (—), symmetric modes (···), $R_1/R_0 = 10$ (◇), $R_1/R_0 = 10/3$ (□), $R_1/R_0 = 2$ (△), $R_1/R_0 = 10/7$ (×), $R_1/R_0 = 10/9$ (○).

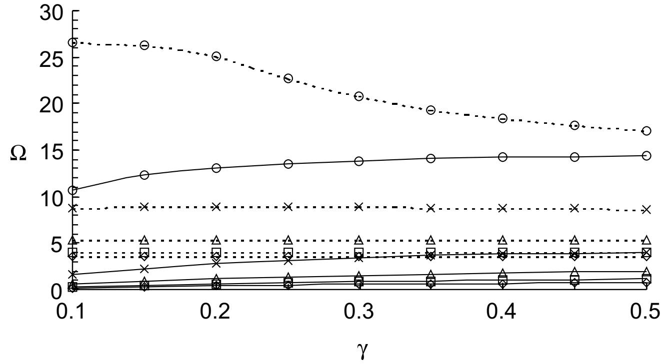

Fig. 3. The fundamental eigenfrequency parameters of axisymmetric vibration ($s = 0^a$) for annular plates with clamped inner edge and free outer edge: antisymmetric modes (—), symmetric modes (···), $R_1/R_0 = 10$ (◇), $R_1/R_0 = 10/3$ (□), $R_1/R_0 = 2$ (△), $R_1/R_0 = 10/7$ (×), $R_1/R_0 = 10/9$ (○).

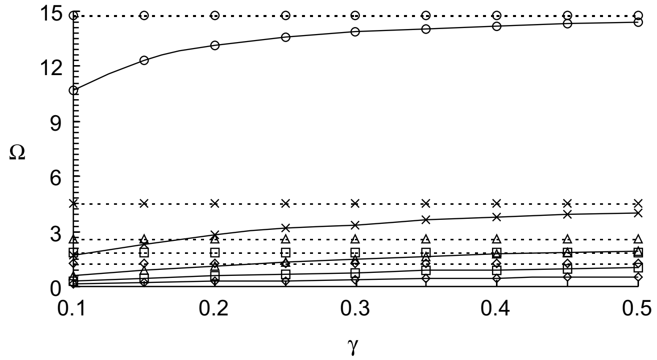

Fig. 4. The fundamental eigenfrequency parameters of circumferential vibration $s = 1$ for annular plates with clamped inner edge and free outer edge: antisymmetric modes (—), symmetric modes (···), $R_1/R_0 = 10$ (◇), $R_1/R_0 = 10/3$ (□), $R_1/R_0 = 2$ (△), $R_1/R_0 = 10/7$ (×), $R_1/R_0 = 10/9$ (○).

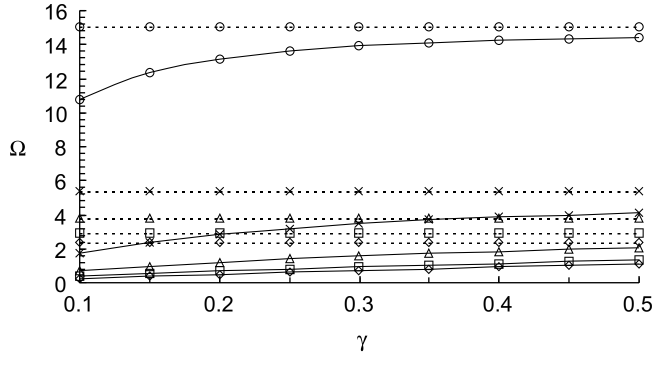

Fig. 5. The fundamental eigenfrequency parameters of circumferential vibration $s = 2$ for annular plates with clamped inner edge and free outer edge: antisymmetric modes (—), symmetric modes (···), $R_1/R_0 = 10$ (◇), $R_1/R_0 = 10/3$ (□), $R_1/R_0 = 2$ (△), $R_1/R_0 = 10/7$ (×), $R_1/R_0 = 10/9$ (○).

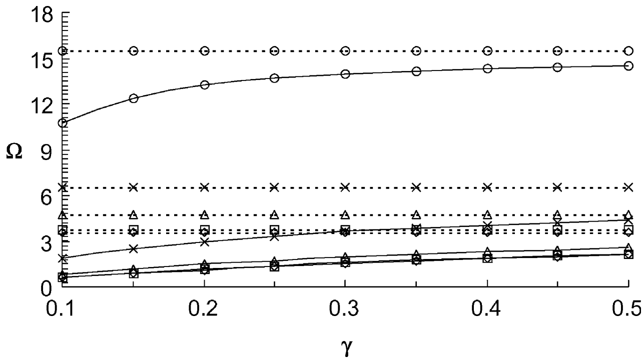

Fig. 6. The fundamental eigenfrequency parameters of circumferential vibration $s = 3$ for annular plates with clamped inner edge and free outer edge: antisymmetric modes (—), symmetric modes (···), $R_1/R_0 = 10$ (◇), $R_1/R_0 = 10/3$ (□), $R_1/R_0 = 2$ (△), $R_1/R_0 = 10/7$ (×), $R_1/R_0 = 10/9$ (○).

antisymmetric mode, when the outer–inner radius ratio R_1/R_0 is above 2, the effect of outer–inner radius ratio on the fundamental eigenfrequencies is very small.

Fig. 3 presents the fundamental eigenfrequency parameters of the antisymmetric and symmetric modes for axisymmetric vibration. It is seen that the fundamental eigenfrequencies of the antisymmetric mode monotonically increase with increasing the thickness–radius ratio. For the symmetric mode, when the outer–inner radius ratio is larger than 10/7, the effect of thickness–radius ratio on the fundamental eigenfrequencies is small. However, when the outer–inner radius ratio is smaller than 10/7, the effect of thickness–radius ratio on the fundamental eigenfrequencies rapidly increases, as for example for $R_1/R_0 = 10/9$. In such a case, the eigenfrequencies monotonically decrease when the thickness–radius ratio increases. Moreover, when the outer–inner radius ratio decreases, both the eigenfrequencies of the antisymmetric and symmetric modes monotonically increase, especially when the outer–inner radius ratio R_1/R_0 is close to 1.

Figs. 4–6 give the fundamental eigenfrequency parameters of the antisymmetric and symmetric modes for circumferential vibrations for $s = 1, 2, 3$. One can see that the effect of thickness–radius ratio on the eigenfrequencies is similar for all three cases. With the increase of the thickness–radius ratio, the eigenfrequencies of the antisymmetric mode monotonically increase. For the symmetric mode, the effect of outer–inner ratio on the fundamental eigenfrequencies is very small. Moreover, when the outer–inner radius ratio decreases, both the eigenfrequencies of the antisymmetric and symmetric modes monotonically increase especially for $R_1/R_0 < 2$.

The study has also covered the effect of thickness–radius ratio on eigenfrequencies of annular plates with free inner edge and clamped outer edge as well as annular plates with both inner and outer edges clamped. The effect of outer–inner radius ratio and thickness–radius ratio on the fundamental eigenfrequencies of each of the vibration categories is generally similar to that for annular plates with clamped inner edge and free outer edge, and therefore the corresponding results are not presented here.

From Figs. 2–6, it is observed that the effect of plate thickness on the fundamental eigenfrequencies of antisymmetric mode is more significant than that of symmetric mode except for the axisymmetric vibration when the plate has an outer–inner radius close to 1. In general, all of the insensitive modes belong to the symmetric modes in the thickness direction. This means that in these modes, the variation of deformation along the plate thickness is very small. These fundamental symmetric modes are mainly dependent on the polar co-ordinate r but not the thickness co-ordinate z, and the deformations u and/or v are predominant while the deformation w is negligible. Such a phenomenon has also been observed and explained by Tzou et al. (1998).

5. Conclusions

The three-dimensional vibration of thick, solid circular and annular plates with the common boundary conditions has been studied, based on the exact, small strain elasticity theory. The governing eigenvalue equation was derived using the Ritz method. In the present analysis, the admissible functions comprise the Chebyshev polynomials multiplied by boundary functions, which ensure the satisfaction of geometric boundary conditions. High accuracy and numerical reliability have been demonstrated through the convergence and comparison study. It is shown that using the Chebyshev polynomials, more eigenfrequencies than using other polynomial functions can be obtained because of the excellent mathematical properties of Chebyshev polynomial series in approximation. The Chebyshev polynomials have an additional advantage in that they can be expressed in terms of cosine functions, which facilitates the analysis and programming. By dividing the vibration of circular plates into three distinct categories and further dividing every category into antisymmetric and symmetric modes, the computational cost can be greatly reduced while maintaining the same level of accuracy. The results show that the thickness–radius ratio has a more remarkable effect on eigenfrequencies of antisymmetric modes in the thickness direction than those of the symmetric modes.

Acknowledgements

The work described in this paper was partially supported by a grant "Three-dimensional vibration analysis of structural components using Chebyshev polynomials" from the University Research Committee (URC) of the University of Honk Kong.

References

Cheung, Y.K., Zhou, D., 2002. Three-dimensional vibration analysis of cantilevered and completely free isosceles triangular plates. International Journal of Solids and Structures 39, 673–687.

Deresiewicz, H., Mindlin, R.D., 1955. Axially symmetric flexural vibrations of a circular disk. ASME Journal of Applied Mechanics 49, 633–638.

Fan, J.R., Ye, J.Q., 1990. Exact solution for axisymmetric vibration of laminated circular plates. ASCE Journal of Engineering Mechanics 116, 20–27.

Fox, L., Parker, I.B., 1968. Chebyshev Polynomials in Numerical Analysis. Oxford University Press, London.

Hanna, N.F., Leissa, A.W., 1994. A higher order shear deformation theory for the vibration of thick plates. Journal of Sound and Vibration 170, 545–555.

Hutchinson, J.R., 1979. Axisymmetric flexural vibrations of a thick free circular plates. ASME Journal of Applied Mechanics 46, 139–144.

Hutchinson, J.R., 1984. Vibration of thick free circular plates, exact versus approximate solutions. ASME Journal of Applied Mechanics 51, 581–585.

Hutchinson, J.R., El-Azhari, S.A., 1986. On the vibration of thick annular plates. In: Refined Dynamical Theories of Beams, Plates and Shells and their Applications. Proceedings of the Euromech-Colloquium 219, pp. 102–111.

Leissa, A.W., 1969. Vibration of Plates, NASA SP-160. Office of Technology Utilization, Washington, DC.

Liew, K.M., Xiang, Y., Kitipornchai, S., 1995. Research on thick plate vibration: a literature survey. Journal of Sound and Vibration 180, 163–176.

Liew, K.M., Yang, B., 1999. Three-dimensional elasticity solutions for free vibrations of circular plates: a polynomials-Ritz analysis. Computer Methods in Applied Mechanics and Engineering 175, 189–201.

Liew, K.M., Yang, B., 2000. Elasticity solutions for free vibrations of annular plates from three-dimensional analysis. International Journal of Solids and Structures 37, 7689–7702.

Liu, C.F., Lee, Y.T., 1997. Axisymmetric straining modes in the vibration of circular plates. Journal of Sound and Vibration 208, 47–54.

Reddy, J.N., 1984. A simple higher-order theory for laminated composite plates. ASME Journal of Applied Mechanics 51, 745–752.

So, J., Leissa, A.W., 1998. Three-dimensional vibrations of thick circular and annular plates. Journal of Sound and Vibration 209, 15–41.

Tzou, K.I., Wickert, J.A., Akay, A., 1998. In-plane vibration modes of arbitrary thick disks. ASME Journal of Vibration and Acoustics 120, 384–391.

Zhou, D., Cheung, Y.K., Au, F.T.K., Lo, S.H., 2002a. Three-dimensional vibration analysis of thick, rectangular plates using Chebyshev polynomial and Ritz method. International Journal of Solids and Structures 39, 6339–6353.

Zhou, D., Au, F.T.K., Lo, S.H., Cheung, Y.K., 2002b. Three-dimensional vibration analysis of a torus with circular cross-section. Journal of the Acoustical Society of America 112, 2831–2840.